Atom-Probe Field-Ion Microscopy Investigation of CMSX-4 Ni-Base Superalloy Laser Beam Welds

S. Babu, S. David, J. Vitek, M. Miller

JOURNAL DE PHYSIQUE IV
Colloque C5, supplément au Journal de Physique III, Volume 6, septembre 1996

Atom-Probe Field-Ion Microscopy Investigation of CMSX-4 Ni-Base Superalloy Laser Beam Welds

S.S. Babu(1), S.A. David, J.M. Vitek and M.K. Miller

Metals and Ceramics Division, Oak Ridge National Laboratory, Oak Ridge, TN 37831-6096, U.S.A.

Abstract: CMSX-4 superalloy laser beam welds were investigated by transmission electron microscopy and atom probe field-ion microscopy (APFIM). The weld microstructure consisted of fine (10- to 50-nm) irregularly shaped γ' precipitates (0.65 to 0.75 volume fraction) within the γ matrix. APFIM compositions of the γ and γ' phases were found to be different from those in the base metal. Concentration profiles across the γ and γ' phases showed extensive variations of Cr, Co and Al concentrations as a function of distance within the γ phase. Calculated lattice misfits near the γ/γ' interface in the welds are positive values compared to the negative values for base metal.

1. INTRODUCTION

Single-crystal Ni-base superalloys are used in both land-based and aerospace turbines due to their excellent high temperature creep-resistant properties. To meet the ever-increasing demand for higher operating temperatures and stresses in modern turbines, new classes of superalloys are being developed by modifying alloy compositions [1]. Changes in alloy composition lead to changes in alloy properties such as single-crystal castability, γ and γ' phase fractions, amount of residual γ-γ' eutectic after solutionizing treatment, recrystallization propensity, carbide phase fraction, alloy density, mechanical and hot-corrosion properties [1]. Single-crystal alloys are also vulnerable to defect formation during processing. Pollack *et al.* related the defect formation to solidification partitioning and solidification cooling rates [2]. The weldability of single-crystal and directionally solidified Ni-base superalloys has gained importance for using the welding process to repair failed components. Nickel aluminide-type alloys have been welded successfully [3-4]. The weld microstructure development of the single-crystal Ni-base superalloys may be complicated due to solidification partitioning and nonequilibrium phase transformations due to rapid cooling and complex alloying additions. Therefore, fundamental understanding of weld-microstructure development is needed and is the subject of a research program [5,6].

The microstructure and solute partitioning in commercial PWA and CMSX series alloys, after standard heat treatments, have been studied previously with atom probe field ion microscopy (APFIM) [7-10]. Electron-beam (EB) welded Ni-base superalloy welds showed only minor differences in solute partitioning compared to that of base metal [6]. However, the effects of rapid weld-cooling conditions on the partitioning characteristics are not known. In general, enhanced weld-cooling conditions are induced by high-energy density processes such as laser welding. To elucidate the welding process effects on the microstructure development and solute partitioning between the γ and γ' phases, laser welds of single-crystal CMSX-4 were investigated with analytical electron microscopy and APFIM. The results are compared with a previous study on EB welding of a PWA-1480 single-crystal Ni-base superalloy. This study is important for welding process design and modeling the development of microstructure during welding of Ni-base single-crystal superalloys.

2. EXPERIMENTAL

Single crystals of CMSX-4 superalloy of composition, Ni-7.5 at. % Cr-0.38% Mo-12.7% Al-9.9% Co-2.1% W-1.3% Ti-2.2% Ta-0.95% Re-0.034% Hf, were studied. This base material showed a typical dendritic pattern and interdendritic segregation in the as-received condition. Autogeneous pulsed laser

(1) On assignment from the Pennsylvania State University, PA 16802.

welds were made on 2- to 3-mm-thick sheets machined from single crystal bars. Full-penetration welds were obtained with laser lamp power, 8.5 to 10 kW, at two welding speeds of 2.1×10^{-3} and 12.7×10^{-3} m s^{-1} referred to as low- and high-speed welds, respectively. The laser pulse rate was set at 40 s^{-1}. During welding, argon was used as a shielding gas to avoid reaction with ambient atmosphere. The welds were examined in the as-welded condition.

The as-welded samples were examined by optical microscopy and in a Philips-CM12 transmission electron microscope with EDX capability. In addition, the Oak Ridge National Laboratory APFIM [11] was used to characterize the partitioning and the possible segregation of alloying elements at γ–γ' interfaces. The samples were imaged at 50 to 60 K with neon, and the atom probe analyses were performed with a residual neon gas pressure of 3×10^{-7} Pa and with a pulse fraction of 20%.

3. RESULTS AND DISCUSSION

In general, optical microscopy of CMSX-4 laser welds showed a fine cellular-dendritic structure. The welds contained equiaxed dendrites. As in the PWA-1480 EB welds, the single-crystallinity could not be maintained in the weld. However, the microstructural features were much finer than those observed in EB welds. A typical low-magnification transmission electron micrograph of low-speed laser weld is shown in Fig. 1. The micrograph revealed a negligible amount of eutectic γ-γ' phase mixture at the solidification cell boundaries. Although the electron diffraction indicated the presence of γ' precipitates, they are difficult to resolve at low magnifications. The γ' precipitates were found to be 10 to 50 nm in size, and the morphologies were found to be irregular and quite different from the classic cuboidal shape [1,12]. The shape of the γ' precipitates is closely related to the chemistry, the lattice misfit between γ and γ' phases and applied stress [13]. Image analysis of the microstructure indicated the volume fraction of γ' phase to be 0.65 to 0.75. Similar microstructures were observed in the case of high-speed welds.

In contrast, interdendritic boundaries in PWA-1480 EB welds were decorated with excessive eutectic γ-γ' phase mixture and Laves phase [6]. In Ni-base superalloys, the eutectic reaction occurs during the final stages of weld solidification. During weld solidification, as the γ phase grows, the liquid enriches with some alloying elements such as Ta, Ti, and Al. Once the enrichment reaches a critical level, satisfying the thermodynamic requirements, a eutectic reaction is initiated, *i.e.*, $\text{liquid} \rightarrow \gamma + \gamma'$. In multicomponent alloys, the eutectic reaction can have a more complicated reaction, such as $\text{liquid} \rightarrow \gamma + \gamma' +$ Laves. The negligible amount of eutectic γ-γ' phase mixture in the present experiment indicates that the solute enrichment in the last solidifying liquid is not sufficient to induce the eutectic reaction.

This lack of enrichment in the liquid can be rationalized as follows. It is known that the partitioning coefficient may change as a function of solidification growth velocity. For example, in iron based alloys, the calculated solidification partitioning coefficient reaches a value of 1 (partitionless solidification) at high solidification growth velocities on the order of 1 ms^{-1} [14]. The high cooling rates in pulsed laser welds will result in high solidification growth velocities that may lead to less enrichment of the liquid, and, consequently, depression of the eutectic reaction.

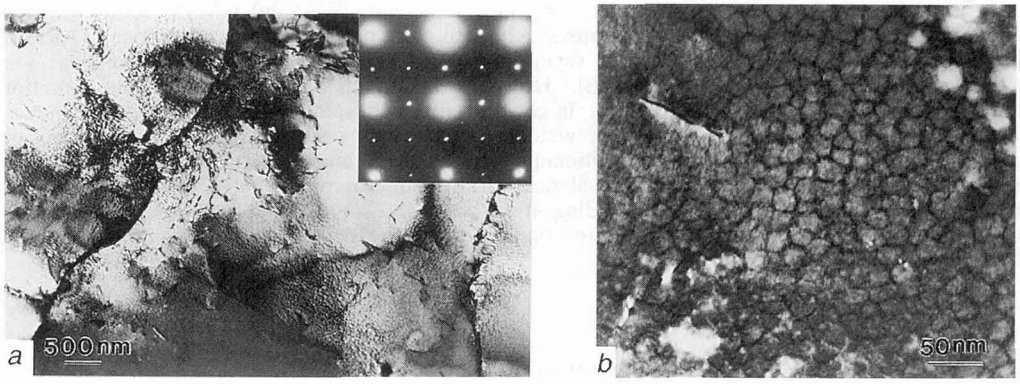

Figure 1. (*a*) Low-magnification micrograph of CMSX-4 low-speed laser weld, showing a solidification cell boundary with a negligible amount of eutectics. Inset shows the electron diffraction pattern indicating the presence of $L1_2$-ordered γ' phase. (*b*) Higher-magnification bright field micrograph illustrating the distribution of fine, irregularly shaped γ' precipitates (10 to 50 nm) within the γ phase.

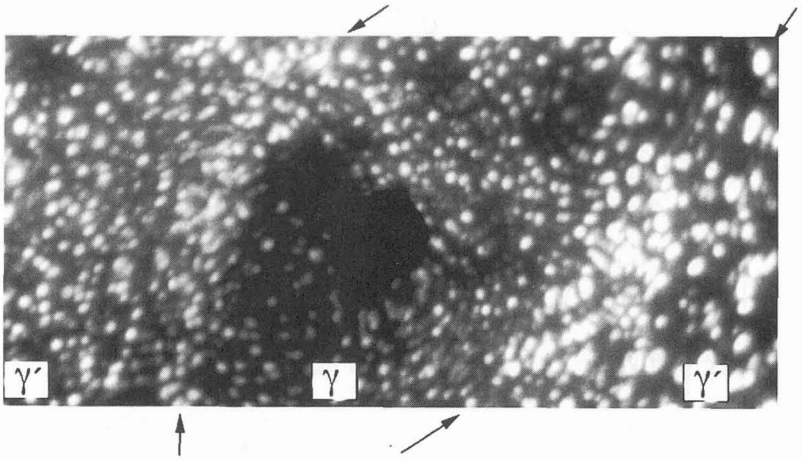

Figure 2. Field-ion image of CMSX-4 low-speed laser weld. Micrograph shows brightly imaging regions of γ' and darkly imaging γ region. The phase boundaries are marked with arrows.

The rapid weld cooling conditions are also expected to change the solid-state decomposition of primary γ phase into γ-γ' phase mixtures. The size of the γ' precipitates in this study (10 to 50 nm) is smaller than those (50 to 500 nm) of the PWA-1480 EB welds [6]. The size difference may be attributed to a high nucleation rate of γ' precipitates due to larger undercooling in the laser welds. In addition to the size difference, it is important to understand the irregular shape of γ' precipitate compared to a classical cuboidal shape. Therefore, the phase compositions and interface concentrations of γ and γ' phases were measured using APFIM.

A field-ion image of CMSX-4 low-speed laser weld, in the as-welded condition, is shown in Fig. 2. The micrograph reveals a darkly imaging γ phase in-between brightly imaging γ' phase regions. Other field-ion images revealed the fine-scale γ and γ' phase distributions. No conclusive indications of solute segregation at the γ/γ' interface based on contrast differences were found in FIM images.

APFIM concentration profiles across the γ and γ' phases (see Fig. 3) showed extensive variations of Cr, Co and Al concentrations as a function of distance in the γ phase. For example, the chromium level in the γ phase near the γ/γ' interface was found to be 15.1 ± 0.2 at. % Cr, compared to 8.6 ± 0.5 at. % Cr in the interior of the γ phase. A small diffusion profile of Ta was also evident in the γ phase. The shapes of the concentration profiles indicate diffusion of Cr and Co (rejected from γ' phase) away from the γ/γ' interface to the interior of γ phase and diffusion of Al and Ta to the γ/γ' interface from the interior of the γ phase. In contrast, the magnitude of concentration variations within γ' phase was smaller. The chromium concentration in γ' phase near the γ/γ' interface was found to be 1.2 ± 0.2 at. % Cr and 1.7 ± 0.2 at. % Cr in the interior of the γ' phase. Small diffusion profiles of W and Ta are also observed in the γ' phase near the interface. The above results suggest a diffusion flux of alloying elements in γ and γ' phases. Blavette *et al.* [9] also measured similar concentration variations in γ' phase in CMSX-2 alloy after standard heat treatments. However, in the present experiment, the magnitudes of concentration variations in the γ phase are larger. Accurate γ/γ' interfacial chemical analysis from high-speed welds has not been obtained. However, the chromium concentration of γ phase (~ 20 at. % Cr) was found to be higher than that of low-speed welds (15 at. % Cr). The reason for the difference is not known and it is speculated that it may be related to the decomposition temperature of γ into γ and γ' phase mixture during weld cooling.

Measured compositions of γ and γ' phases in low-speed welds are compared with published compositions [15] in Table 1. The comparison suggests that the γ and γ' phase mixtures in the laser weld are quite different from that of base metal values. However, the concentration profiles support a diffusional redistribution of alloying elements between γ and γ' phases at a particular temperature to reach equilibrium. Due to rapid weld cooling, the distribution was not completed and the concentration profiles at a higher temperature were frozen. The diffusional redistribution is expected to reach completion at service temperature or during post-weld heat treatment (PWHT). However, the path of this compositional redistribution is expected to be complex and depends upon the equilibrium compositions of γ and γ' phases. Implications of such a large concentration variation observed in the as-welded state are analyzed in detail.

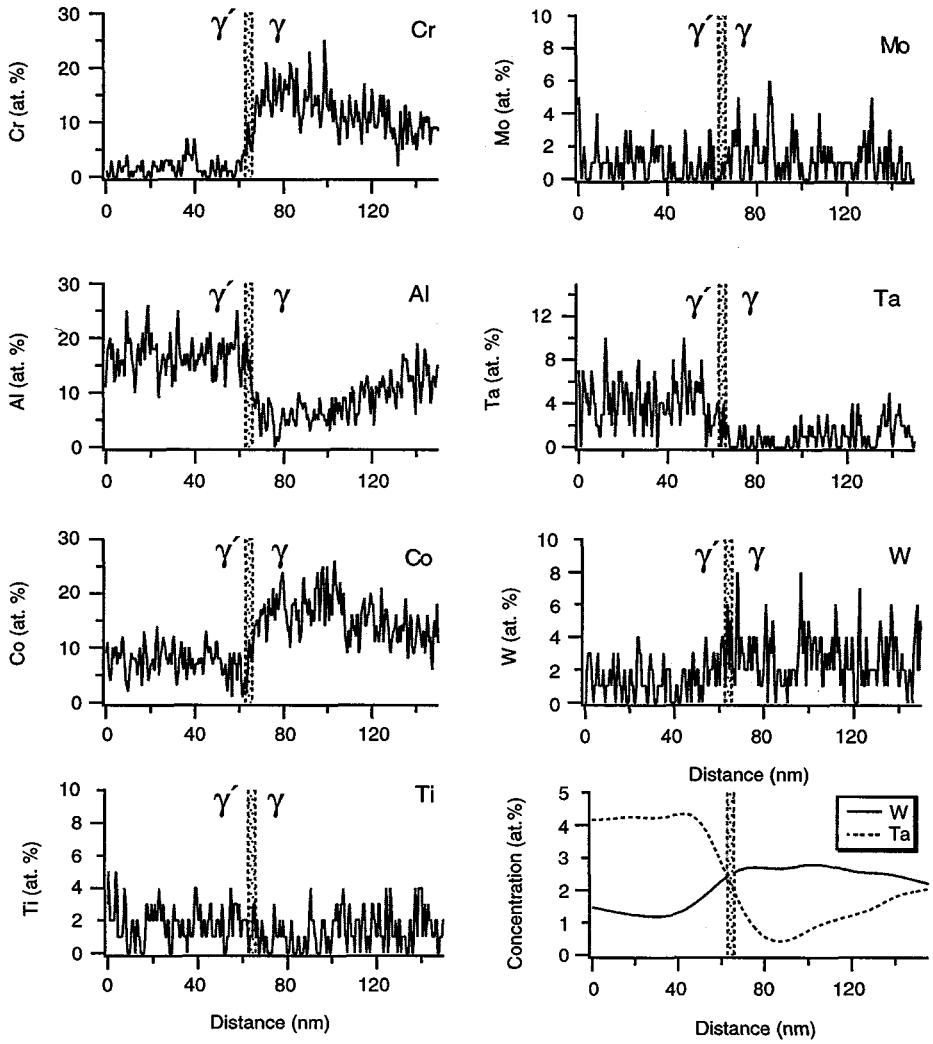

Figure 3. The APFIM concentration profile obtained across γ and γ´ phases from the CMSX-4 low-speed laser weld. The plots also show a smoothed concentration profiles of W and Ta to illustrate the shape of concentration gradients.

Table 1. Comparison of γ and γ´ phase compositions (in at. %) in low-speed laser welds with the published data [15]. In this table **B** and **I** correspond to bulk and interface, respectively. Since the compositions were presented in a graph, the error estimates were not reported in the reference 17.

Phase	Al	Ti	Cr	Co	Mo	Hf	Ta	W	Re
γ [17]	8.7	1.5	12.9	15.0	1.25	0	0.83	5.0	4.6
γ (**B**)	12.6±0.6	1.6±0.2	8.6±0.5	12.5±0.6	1.0±0.2	0	1.8±0.2	2.6±0.3	0.9±0.2
γ (**I**)	5.4±0.4	0.8±0.2	15.1±0.7	16.9±0.7	1.7±0.2	0	0.5±0.1	2.5±0.3	1.8±0.2
γ´ [17]	12.36	3.3	3.71	7.83	0	0	3.38	1.65	0.08
γ´ (**B**)	17.0±0.6	1.7±0.2	1.7±0.2	7.9±0.4	1.2±0.2	0.03±0.03	4.2±0.3	1.3±0.2	0.1±0.05
γ´ (**I**)	16.9±0.8	1.7±0.3	1.2±0.2	7.4±0.5	0.6±0.2	0	4.6±0.4	1.5±0.2	0.2±0.1

The measured compositions of γ and γ' phases, excluding the interface compositions, were used to estimate the volume fraction of γ' phase in the laser welds. The volume fraction is estimated using the lever rule and by a method used by Blavette *et al.* [9] in which all the ratios of $(C_n - C_\gamma) / (C_{\gamma'} - C_\gamma)$ for all elements are plotted. The parameters C_n, C_γ, and $C_{\gamma'}$ are the nominal, γ phase, and γ' phase concentrations, respectively. The slope of the best-fit line passing through the origin for all these ratios gives an estimate of volume fraction. The estimated volume fraction of γ' phase (0.55) in low-speed welds (see Fig. 4*a*) is lower than the estimated volume fraction in high-speed welds (0.71) and that of the base metal (0.67) [15]. Microstructural measurements on both the high- and low-speed welds yielded volume fractions of ~ 0.65 to 0.75. Since these estimates do not consider the concentration variations in γ phase (see Fig. 3), the volume fraction values can not be directly compared with experimental measurements. It is expected that the volume fractions of γ' phase are expected to vary as a function of diffusional redistribution. The estimated volume fractions support the tendency for such a change in laser welds during service or PWHT.

The shape of the γ' precipitates depends on the lattice misfit between γ and coherent γ' phase, because it contributes to the lattice strains. The irregular morphology of γ' precipitates in the laser welds can be rationalized if there is a change in lattice misfit parameter. Lattice misfit for the welds and the published base metal composition [15] are estimated. The lattice misfit percentage is given by:

$$100 \times (a_{\gamma'} - a_\gamma)/[(a_{\gamma'}+a_\gamma)/2], \quad (1)$$

where a_γ, and $a_{\gamma'}$ are the lattice parameters of the γ and γ' phase, respectively. The lattice parameters were estimated from the interface compositions and with a published procedure [16]. The estimated misfit values of the laser welds are positive compared to the negative values for the base metal. The observed irregular shape of the γ' phase may be related to this excessively large positive misfit.

These misfit values are expected to change as the redistribution of alloying elements between γ and γ' phase continues during high-temperature aging. For example, the γ' precipitate morphology in CMSX-4 alloys changes and attains an elongated "raft" like morphology during service stress and temperature conditions [17]. This raft-like structure is known to be resistant to creep under low stresses at high temperature. The rafting behavior is related to the lattice strains created due to the negative lattice misfit between γ and γ' phases and stress conditions [17]. Such a morphological change in laser welds under stress during service may be complicated due to elemental redistribution between γ and γ' phases. As the elemental redistribution occurs, the interface concentration may change. This change will lead to a change in lattice misfit and subsequent morphological change. However, predictions of the rate and extent of elemental distribution between γ and γ' phases, and the resulting changes in lattice misfit and the morphology, are not possible. Moreover, the shape changes due to service-stress and temperature conditions are expected to be complex and need further investigation.

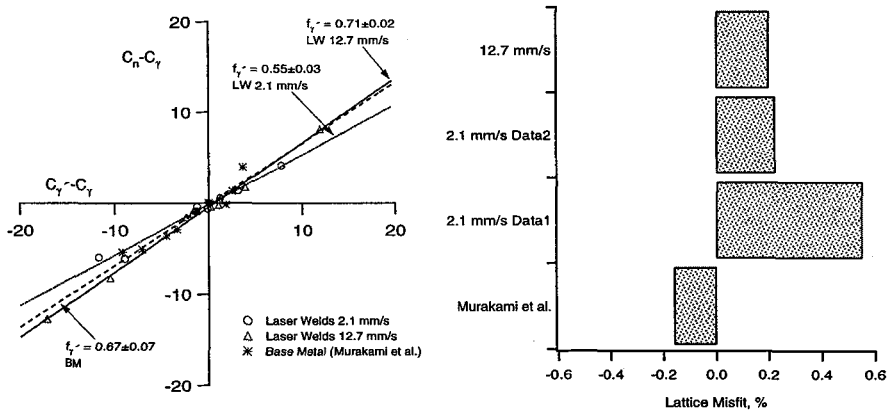

(*a*) (*b*)

Figure 4. Various methods of comparing the measured APFIM composition of γ and γ' phases from low- and high-speed welds with published data (*a*) comparison of estimated volume fraction of γ and γ' phases and (*b*) comparison of calculated lattice misfit using the measured interface composition of γ and γ' phases. Data1 and Data2 correspond to two different interface concentrations. Since the interface concentrations from high-speed welds are not accurate, the lattice parameter misfit values must be considered as approximate.

4. Summary and Conclusions

The microstructure development and partitioning of alloying elements between γ and γ' phases were investigated in CMSX-4 superalloy laser welds. Transmission electron microscopy revealed fine (10 to 50 nm) irregularly shaped γ' (0.65 to 0.75 volume fraction) precipitates whose morphology was distinctly different from the cuboidal shape. There was a negligible amount of eutectic γ-γ' phase mixture at the solidification cell boundaries. FIM images also revealed fine γ and γ' phases, and APFIM compositions of γ and γ' phases were found to be different from that of base metal. Concentration profiles across γ and γ' phases showed extensive concentration variations of Cr, Co and Al as a function of distance within the γ phase. The calculated lattice misfit percentage was found to be significantly different from that expected from the composition of γ and γ' phases in the base metal. The elemental redistribution during high-temperature exposure may modify the lattice misfit, morphology, and volume fraction γ' precipitates. In summary, the results suggest that, during welding, γ phase formed from the liquid by rapid solidification, and during subsequent cooling, this γ phase decomposed into the γ and γ' two-phase mixtures with non-equilibrium redistribution of alloying elements.

Acknowledgments

This research was sponsored by the Division of Materials Sciences, U.S. Department of Energy, under contract DE-AC05-96OR22464 with Lockheed Martin Energy Research Corporation. The authors thank Dr. M. Burke of Westinghouse Electric Corporation for providing the CMSX-4 alloys, R. W. Reed and K. F. Russell for technical assistance, K. Spence for editing, and Drs. M. L. Santella and A. J. Duncan for helpful discussions. This research was conducted utilizing the Shared Research Equipment (SHaRe) User Program facilities at Oak Ridge National Laboratory.

References

[1] Harris K., Erickson G. L., Sikkenga S. L., Brentnall W. D., Aurrecoechea J. M., and Kubarych K. G., "Superalloys 1992", Seven Springs, PA, 1992, S. D. Antolovich, R. W. Stusrud, and R. A. MacKay, D. L. Anton, T. Khan, R. D. Kissinger, and D. L. Klarstrom Eds. (The Minerals, Metals & Materials Society, Warrendale, PA, 1992) pp. 297-306.
[2] Pollack T. M., Murphy W. H., and Goldman E. H., Uram D. L., and Tu J. S., "Superalloys 1992," Seven Springs, PA, 1992, S. D. Antolovich, R. W. Stusrud, R. A. MacKay, D. L. Anton, T. Khan, R. D. Kissinger, and D. L. Klarstrom Eds. (The Minerals, Metals & Materials Society, Warrendale, PA, 1992) pp. 125-134.
[3] Santella M. L., *Scr. Metall. . Mater.* **28** (1993) 1305-1310.
[4] Santella M. L., and David S. A., *Welding J.* **65** (1986) 129s-137s.
[5] David S. A., Vitek J. M., Babu S. S., Boatner L. A., and Reed R. W., submitted for publication in *Science and Technology of Welding and Joining*, 1996.
[6] Babu S. S., David S. A., and Miller M. K., *Appl. Surf. Sci.* **94/95** (1996) 280-287.
[7] Miller M. K., Jayaram R., Lin L. S., and Cetel A. D., *Appl. Surf. Sci.* **76/77** (1994) 172-176.
[8] Blavette D., Bostel A., and Sarrau J. M., *Metall. Trans. A.* **16A** (1985) 1703-1711.
[9] Blavette D., Caron P., and Khan T., "Superalloys 1988", Seven Springs, Seven Springs, PA, 1988, S. Reichman, D. N. Duhl, G. Maurer, S. Antolovich, and C. Lund Eds. (The Minerals, Metals & Materials Society, Warrendale, PA, 1988) pp. 305-314.
[10] Wanderka N., and Glatzel U., *Mater. Sci. Eng.* **A203** (1995) 69-74.
[11] Miller M. K., *J. de Phys.* **C2-47** (1986) 493-499.
[12] Sengupta A., Putatunda S. K., Bartosiewicz L., Hangas J., Nailos P. J., Peputapeck M., and Alberts F. E., *JMEPEG* **3** (1994) 664-672.
[13] Peng Z., Glatzel U., Link T., and Feller-Knoepmeier M., *Scr. Mater.* **34** (1996) 221-226.
[14] Kurz, W., "Proceedings of 4th International Conference on Trends in Welding Research," Gatlinburg, Tennessee, June 5-8, 1995, H. B. Smartt, J. A. Johnson, and S. A. David Eds. (ASM, Materials Park, Ohio, 1995).
[15] Murakami H., Harada H., and Bhadeshia H. K. D. H., *Appl. Surf. Sci.* **76/77** (1994) 177-183.
[16] Harada H., and Yamazaki M., *Tetsu to Hagañe* **65** (1979) 337-346.
[17] Nabarro F. R. N., *Metall. Mater. Trans. A* **27A** (1996) 513-530.